

Responses of *Phanerochaete chrysosporium* to Toxic Pollutants: Physiological Flux, Oxidative Stress, and Detoxification

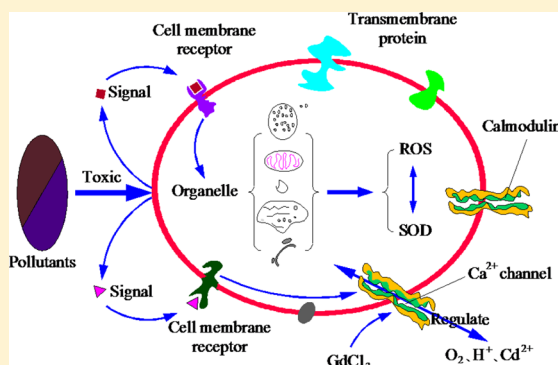
Guang-Ming Zeng,^{*,†,‡} An-Wei Chen,^{†,‡} Gui-Qiu Chen,^{*,†,‡} Xin-Jiang Hu,^{†,‡} Song Guan,^{†,‡} Cui Shang,^{†,‡} Lun-Hui Lu,^{†,‡} and Zheng-Jun Zou^{†,‡}

[†]College of Environmental Science and Engineering, Hunan University, Changsha 410082, P.R. China,

[‡]Key Laboratory of Environmental Biology and Pollution Control (Hunan University), Ministry of Education, Changsha 410082, P.R. China

S Supporting Information

ABSTRACT: The white-rot fungus *Phanerochaete chrysosporium* has been widely used for the treatment of waste streams containing heavy metals and toxic organic pollutants. The development of fungal-based treatment technologies requires detailed knowledge of the relationship between bulk water quality and the physiological responses of fungi. A noninvasive microtest technique was used to quantify real-time changes in proton, oxygen, and cadmium ion fluxes following the exposure of *P. chrysosporium* to environmental toxic (2,4-dichlorophenol and cadmium). Significant changes in H⁺ and O₂ flux occurred after exposure to 10 mg/L 2,4-dichlorophenol and 0.1 mM cadmium. Cd²⁺ flux decreased with time. Reactive oxygen species formation and antioxidant levels increased after cadmium treatment. Superoxide dismutase activity correlated well with malondialdehyde levels ($r^2 = 0.964$) at low cadmium concentrations. However, this correlation diminished and malondialdehyde levels significantly increased at the highest cadmium concentration tested. Real-time microscale signatures of H⁺, O₂, and Cd²⁺ fluxes coupled with oxidative stress analysis can improve our understanding of the physiological responses of *P. chrysosporium* to toxic pollutants and provide useful information for the development of fungal-based technologies to improve the treatment of wastes cocontaminated with heavy metals and organic pollutants.



INTRODUCTION

As one of the most effective methods for environmental remediation, bioremediation has increasingly attracted the attention of environmentalists.¹ Bioremediation using microorganisms offers an attractive treatment option because this technology is cost-effective, environmentally compatible, and has high removal efficiency for various pollutants.^{1–3} A large number of microorganisms have been the focus of research for their potential pollutant disposal ability. White-rot fungi are the most efficient lignin degraders, and the representative species, *Phanerochaete chrysosporium*, has been extensively used for its ability to degrade a wide range of organic substrates.^{4–6} Generally, the organic substrates degraded by *P. chrysosporium* may coexist with heavy metals in wastewater, which can affect microbial reproduction and cause morphological and physiological changes.^{7,8}

The biodegradation or biosorption ability of microorganisms may deteriorate due to the morphological and physiological changes caused by heavy metals and toxic organic pollutants in the environment.^{9,10} For example, cadmium causes cellular toxicity via several mechanisms, including interference with DNA repair and protein metabolism, membrane lipid peroxidation, physiological Zn(II) substitution, and reactive oxygen species (ROS) formation.^{11,12} Oxygen free radicals,

such as hydrogen peroxide (H₂O₂), superoxide (O₂⁻), and hydroxyl (OH⁻) radicals, are among the most reactive compounds induced by heavy metal stress.¹³ Excess free radicals could lead to multiple toxic effects, such as lipid peroxidation, protein cleavage, and DNA damage.^{14,15}

Removal of toxic pollutants from substrates is a challenge because they affect fungal colonization and bioactivity.¹⁶ It is necessary to understand the interactions between *P. chrysosporium* and the pollutants in the medium. Previous studies have shown that *P. chrysosporium* can tolerate heavy metals and toxic organic pollutants to some degree and remove them from wastewater.^{17–19} It is likely that multiple mechanisms, such as efflux pumps, modifying enzymes, target mutations, and resistance systems, are involved in microbial resistance to environmental stress (e.g., UV radiation or chemical toxic exposure).^{20–22} Therefore, *P. chrysosporium* can adapt to complex polluted environments.

Although *P. chrysosporium* studies on organic matter degradation and metal accumulation from liquid media can

Received: March 14, 2012

Revised: June 8, 2012

Accepted: June 15, 2012

Published: June 15, 2012

provide useful information on the relationship between fungal activities and pollutants,^{3,23} they do not accurately reflect the treatment process. Our previous study also demonstrated a decrease in the pH of the treatment system (from 6.5 to 3.6) and cadmium concentration-dependent alterations in protein production and enzymatic activities of *P. chrysosporium*;³ however, the underlying mechanisms remain unknown. To date, the effects of pollutant stress on the metabolism, resistance, and adaptive responses of *P. chrysosporium* have not been reported in the literature. Particularly, the effects of toxic pollutants on the physiological flux, oxidative stress, and detoxification of *P. chrysosporium* have not been investigated. The relative toxicities and fates of pollutants occurring in the growth environment of *P. chrysosporium* remain unknown. From an environmental point of view, it is important to understand the responses of *P. chrysosporium* to toxic pollutants. Such information would enable the development of fungal-based technologies to improve the removal of metal-polluted organic wastes.

Therefore, the main purpose of this study was to examine the responses of *P. chrysosporium* to toxic pollutants using physiological measurements. We tested the toxic organic pollutant 2,4-dichlorophenol (2,4-DCP) and the heavy metal cadmium, which are typically found in sites cocontaminated with organic and heavy metal pollutants. To assess physiological responses, we monitored real-time changes in H⁺, O₂, and Cd²⁺ fluxes in *P. chrysosporium* following exposure to pollutants using noninvasive microtest technology. Further, antioxidative responses of *P. chrysosporium* to cadmium were also evaluated. These studies would help clarify the mechanisms involved in heavy-metal toxicity and/or elucidate the cellular basis of mass tolerance to these compounds.

MATERIALS AND METHODS

Strain and Chemicals. The *P. chrysosporium* strain BKMF-1767 (ATCC 24725) was obtained from the China Center for Type Culture Collection (Wuhan, China). Stock cultures were maintained on malt extract agar slants at 4 °C. Spores were gently scraped from the agar surface and blended in sterile distilled water to obtain a spore suspension. The spore concentration was adjusted to 2.0 × 10⁶ spores/mL. Aqueous suspensions of fungal spores were inoculated into Kirk's liquid culture medium²⁴ in 500-mL Erlenmeyer flasks. All the chemicals used in this study were of analytical reagent grade.

Physiological Flux. After 3 days of growth in liquid medium, *P. chrysosporium* pellets were harvested and exposed to toxics. Net fluxes of H⁺, O₂, and Cd²⁺ were measured using the noninvasive microtest technique (the NMT system BIO-IM; YoungerUSA, LLC, Amherst, MA) and the Optical Oxygen Flux Measurement System (YG00-01A; YoungerUSA) at Xuyue (Beijing) Science & Technology Co. Ltd., China (SI Figure S1). A schematic of *P. chrysosporium* H⁺, O₂, and Cd²⁺ flux measurements using microelectrodes is shown in SI Figure S2. The principle of NMT and its applications in ion flux detection have been described previously.^{25–27} Briefly, for H⁺ and Cd²⁺ flux measurements, prepulled and silanized glass micropipets (inner diameter, 3 ± 1 μm; XYPG120–2; Xuyue) were first filled with a backfilling solution (H⁺: 15 mM NaCl + 40 mM KH₂PO₄ at pH 7.0; Cd²⁺: 10 mM CdCl₂ + 0.1 mM KCl) to a distance of ~1 cm from the tip. The micropipets were then front-filled with approximately 30 μm-columns of selective liquid ion-exchange cocktails (Hydrogen ionophore I-cocktail B [Product No. 95293]; Cadmium Ionophore I,

[Product No. 20909]; Sigma-Aldrich, St Louis, MO). Ion-selective electrodes were calibrated prior to flux measurements with different concentrations of target ion buffer (H⁺: pH 4.5 and 6.5; Cd²⁺: 0.05 and 0.5 mM). Only electrodes with Nernstian slopes greater than a certain value per decade (H⁺: 58 mV; Cd²⁺: 25 mV) were used in this study. The concentration gradients of the target ions were measured by moving the ion-selective microelectrode between 2 points close to the fungal pellet surface (ca. 3 ± 1 μm) in a preset excursion with a distance of 30 μm. During the measurement of Cd²⁺ flux, *P. chrysosporium* cells were treated with a Ca²⁺ channel inhibitor (GdCl₃, 0.1 mM), and changes in Cd²⁺ flux before and after the treatment were recorded.

For O₂ flux measurement, fiber-optic oxygen microsensors (optrodes) and a frequency-domain lifetime fluorometer were constructed using previously published techniques.²⁸ Optrodes (tip diameter, 5–7 μm) were calibrated in sterile nitrogen-purged and O₂-saturated growth media (21%). The measured phase angle was transduced to an analog signal via a digital signal processor (YG00-MC; YoungerUSA).^{29,30} The recording rate for the H⁺ and Cd²⁺ fluxes was 5.96 s/reading. For O₂, the entire cycle was completed in 8.91 s. Ionic/molecular fluxes were calculated using Fick's law of diffusion

$$J = -D \frac{dc}{dx}$$

where J represents the ion flux in the x direction, and dc/dx is the ion concentration gradient. In our experiments, dx was 30 μm, which is the distance of the microelectrode movement between a close point and far point, and D is the ion diffusion coefficient (varying with the kind of ion) in a particular medium. Data and image acquisition, preliminary processing, control of the electrode position, and stepper motor-controlled fine focus of the microscope stage were performed with the imFlux software. All experiments were repeated 5 times to ensure the validity of physiological trends.

Antioxidant Enzymes. Superoxide dismutase (SOD) activity was measured according to the method reported by Choudhary et al.³¹ The cells were harvested by centrifugation and homogenized in 0.05 M phosphate buffer (pH 7.8). The homogenate was centrifuged at 15,000 rpm at 4 °C, and the supernatant was used for enzyme assay. SOD activity was assayed by monitoring the inhibition of photochemical reduction of nitroblue tetrazolium chloride (NBT) in a reaction mixture containing 1 M Na₂CO₃, 200 mM methionine, 2.25 mM NBT, 3 mM EDTA, 60 mM riboflavin, and 0.1 M phosphate buffer (pH 7.8). Absorbance was read at 560 nm.

Catalase (CAT) activity was measured in a 3-mL reaction mixture containing 50 μL of enzymatic extract, 20 mM H₂O₂, and 50 mM potassium phosphate buffer (pH 7.0), according to the method reported by Cavalcanti et al.³² The disappearance of H₂O₂ was evaluated by measuring the decrease in absorbance at 240 nm (molar extinction coefficient $\epsilon = 36.6 \text{ mM}^{-1} \text{ cm}^{-1}$).

Lipid Peroxidation and Superoxide (O₂⁻) Production. Lipid peroxidation was evaluated by measuring the concentration of malondialdehyde (MDA), which is a cytotoxic product of lipid peroxidation and an indicator of free radical production and consequent tissue damage.³¹ MDA content was estimated using the procedure described by Aravind and Prasad,³³ with minor modifications. The harvested *P. chrysosporium* cells were homogenized in 10% trichloroacetic acid and centrifuged at 10,000 rpm for 15 min. The supernatant was boiled with thiobarbituric acid for 20 min. The heated

supernatant was centrifuged at 5000 rpm for 5 min, and the absorbance was measured at 532 and 600 nm using the UV-visible spectrometer, Specord 200 PC.

O_2^- production was analyzed as described by Lei et al.³⁴ The harvested cells were homogenized in 2 mL of 50 mM potassium phosphate buffer (pH 7.8) and centrifuged at 10,000 rpm for 10 min at 4 °C. One milliliter of the supernatant was mixed with 0.9 mL of 50 mM potassium phosphate buffer (pH 7.8) and 0.1 mL of 10 mM hydroxylamine hydrochloride. The reaction mixture was incubated at 25 °C for 20 min before adding 1 mL of 17 mM p-aminobenzenesulfonic acid and 1 mL of 7 mM α -naphthylamine. After further incubation (25 °C, 20 min), the absorbance of the mixture was spectrophotometrically recorded at 530 nm.

Statistical Analysis. The mean changes in H^+ , O_2 , and Cd^{2+} fluxes were calculated by averaging continuous flux measurements during pre-exposure and peak exposure. The results are presented as the mean of 5 replicates, and standard deviations were used to analyze experimental data. A one-way analysis of variance (ANOVA) was used to test for significant differences ($\alpha < 0.05$) between the flux values for each treatment. All reported error bars represent one standard error of the arithmetic mean.

RESULTS

Chemical Toxic Exposure and Stress Response.

Representative real-time plots of *P. chrysosporium* H^+ and O_2 fluxes during exposure to 2,4-DCP and cadmium are presented in Figure 1A (for the average value around the fungal surface, see Figure 1B). After exposure to 2,4-DCP (10 mg/L), the H^+ influx increased compared with the pre-exposure value (pre-exposure: -33 ± 4 $\text{pmol cm}^{-2} \text{s}^{-1}$; peak stress response: -37 ± 3 $\text{pmol cm}^{-2} \text{s}^{-1}$; throughout the manuscript, negative and positive values represent influx and efflux, respectively). The oxygen flux of *P. chrysosporium* initially increased upon exposure to 10 mg/L 2,4-DCP (4 ± 0.5 min) and subsequently decreased; the stable O_2 influx of *P. chrysosporium* after exposure to 2,4-DCP was higher than the pre-exposure value. The stable O_2 flux values during pre-exposure and exposure were -44 ± 0.5 and -45 ± 1 $\text{pmol cm}^{-2} \text{s}^{-1}$, respectively. These results were different from those for *Nitrosomonas europaea* biofilm during chlorocarbonyl cyanide phenylhydrazone exposure.²² After the subsequent addition of 0.1 mM $Cd(NO_3)_2$, the H^+ flux changed from influx to efflux (13 ± 5 $\text{pmol cm}^{-2} \text{s}^{-1}$). The O_2 efflux rapidly decreased, indicated by the high slope of the O_2 influx plot in Figure 1A, after the addition of 0.1 mM $Cd(NO_3)_2$. The monitored real-time H^+ and O_2 fluxes following sequential exposure *P. chrysosporium* to 2,4-DCP or Cd^{2+} only are presented in SI Figures S3–S5, and the results are described in the Supporting Information.

The Cd^{2+} flux of *P. chrysosporium* after exposure to 0.1 mM $Cd(NO_3)_2$ is shown in Figure 2. An obvious Cd^{2+} influx (-66 ± 2 $\text{pmol cm}^{-2} \text{s}^{-1}$) into *P. chrysosporium* pellets was observed in the initial 15 ± 0.2 min of exposure. The following two reasons may account for this phenomenon: adsorption of Cd^{2+} by *P. chrysosporium* mycelia and entry into the cells following penetration of the cell wall and plasma membrane. Subsequent addition of 0.1 mM $GdCl_3$ (Ca^{2+} channel inhibitor)^{35–37} elicited a dramatic decrease in Cd^{2+} influx from -66 ± 2 $\text{pmol cm}^{-2} \text{s}^{-1}$ to -45 ± 3 $\text{pmol cm}^{-2} \text{s}^{-1}$, indicating that Ca^{2+} channels were involved in Cd^{2+} influx.

Figure 3 demonstrates the Cd^{2+} flux of *P. chrysosporium* in response to different durations of 0.1 and 0.5 mM $Cd(NO_3)_2$

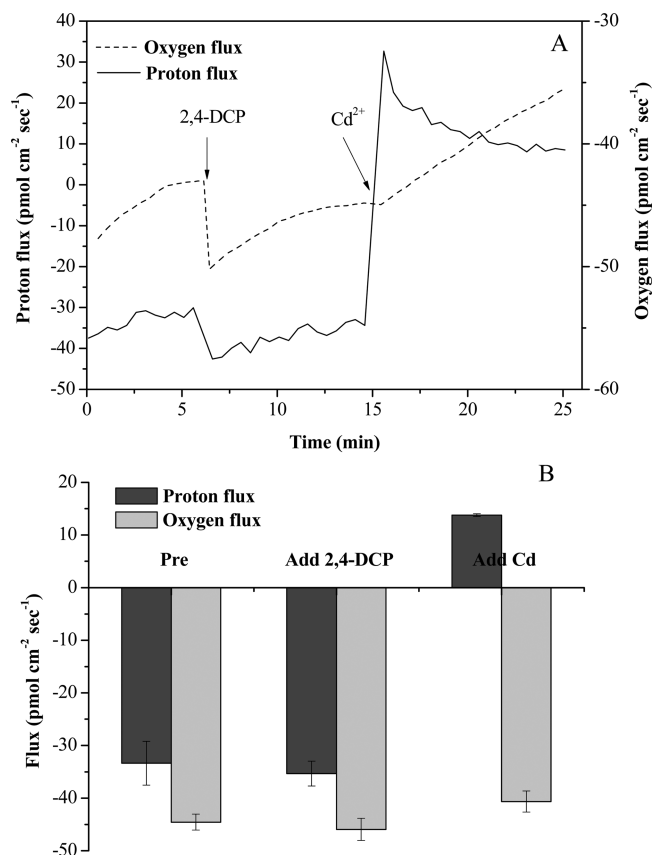


Figure 1. Proton and oxygen fluxes of *P. chrysosporium* during exposure to 10 mg/L 2,4-DCP and 0.1 mM $Cd(NO_3)_2$. (A) Representative real-time plots. (B) Average values at the fungal surface. “Pre” means pre-exposure.

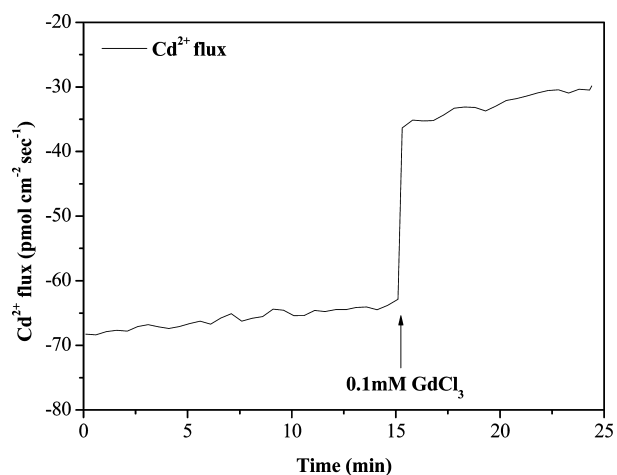


Figure 2. Real-time Cd^{2+} flux of *P. chrysosporium* during exposure to 0.1 mM $Cd(NO_3)_2$ and 0.1 mM $GdCl_3$.

treatment. The Cd^{2+} flux of *P. chrysosporium* following treatment with 0.1 mM $Cd(NO_3)_2$ at 0, 1, 3, and 6 h were -65 ± 4 , -20 ± 1 , -6 ± 0.2 , and 0.2 ± 0.7 $\text{pmol cm}^{-2} \text{s}^{-1}$, respectively. The Cd^{2+} influx decreased with the duration of exposure, which reflects a gradual saturation of the adsorption and uptake processes. A similar trend was observed when 0.5 mM $Cd(NO_3)_2$ was used. The Cd^{2+} flux exhibited a small efflux (0.2 ± 0.7 $\text{pmol cm}^{-2} \text{s}^{-1}$) and a small influx (-0.1 ± 1.5 $\text{pmol cm}^{-2} \text{s}^{-1}$) at the 6 h time point of treatment with 0.1 mM and

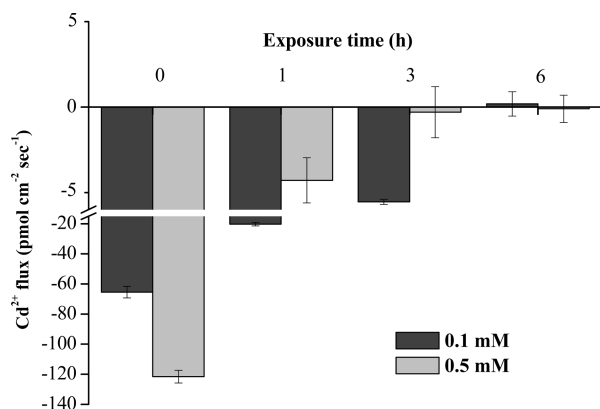


Figure 3. Cd^{2+} fluxes of *P. chrysosporium* in response to different durations of treatment with 0.1 and 0.5 mM $\text{Cd}(\text{NO}_3)_2$. Numbers on the abscissa represent the exposure time. “0 h” indicates the measurement of Cd^{2+} flux immediately after exposure.

0.5 mM $\text{Cd}(\text{NO}_3)_2$, suggesting that equilibrium was achieved and the Cd^{2+} flux was in a state of dynamic equilibrium (SI Figures S6 and S7). Similar results were found when studying BY-2 cells Cd^{2+} flux following exposure to 150 μM Cd^{2+} .³⁸ In the present study, 0.5 mM $\text{Cd}(\text{NO}_3)_2$ elicited a Cd^{2+} influx of -121 ± 4 $\text{pmol cm}^{-2} \text{s}^{-1}$, which was higher than that following treatment with 0.1 mM $\text{Cd}(\text{NO}_3)_2$. However, when the *P. chrysosporium* pellets were exposed to 0.5 mM $\text{Cd}(\text{NO}_3)_2$ for 1 h, the Cd^{2+} influx dramatically decreased to -5 ± 1 $\text{pmol cm}^{-2} \text{s}^{-1}$, which was lower than that following a 1-h treatment with 0.1 mM $\text{Cd}(\text{NO}_3)_2$. This may be attributed to different driving forces and Cd^{2+} toxicity in *P. chrysosporium*.

The percent changes in flux of *P. chrysosporium* pellets following exposure to 2,4-DCP and $\text{Cd}(\text{NO}_3)_2$ are shown in Figures S8 and 4. All physiological stress responses were

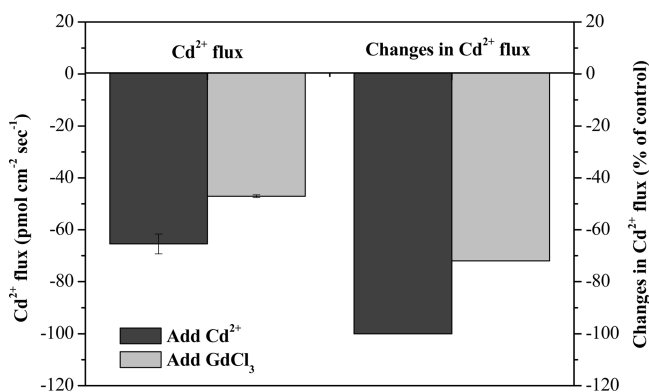


Figure 4. Average Cd^{2+} flux and change in Cd^{2+} flux of *P. chrysosporium* during exposure to 0.1 mM $\text{Cd}(\text{NO}_3)_2$ and 0.1 mM GdCl_3 .

significantly different from those of null controls. After the addition of 2,4-DCP, O_2 and H^+ fluxes increased by 3% and 6% respectively, relative to pre-exposure levels. Upon addition of 0.1 mM $\text{Cd}(\text{NO}_3)_2$, the H^+ flux shifted from influx (-37 ± 3 $\text{pmol cm}^{-2} \text{s}^{-1}$) to efflux (13 ± 5 $\text{pmol cm}^{-2} \text{s}^{-1}$). The average oxygen flux decreased by 9% in the initial 10 ± 0.5 min of exposure. A larger reduction ($30 \pm 1\%$) in Cd^{2+} influx was observed following treatment with 0.1 mM gadolinium (GdCl_3), which is known to block stretch-activated calcium

channels, indicating the involvement of extracellular cadmium influx via these channels.

Cd^{2+} -Induced Oxidative Stress and Detoxification.

The biological responses to cadmium exposure are presented in Figure 5. Enzymatic activities and ROS levels were

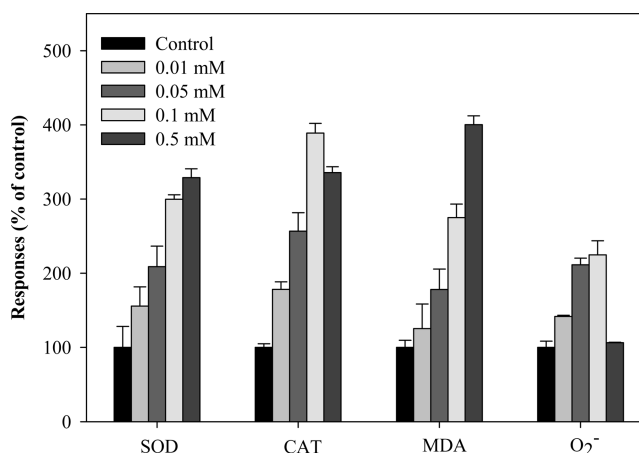


Figure 5. Biological responses of *P. chrysosporium* to various concentrations of $\text{Cd}(\text{NO}_3)_2$. A 3-day-old culture was treated with 0, 0.01, 0.05, 0.1, or 0.5 mM $\text{Cd}(\text{NO}_3)_2$ solution and further cultivated for 2 h. The cells were then collected and washed twice with distilled water for the above analysis.

significantly altered in the cadmium-treated group compared to control (untreated group). SOD activity and MDA content increased in a concentration-dependent manner after exposure to cadmium solution. Another antioxidant enzyme, CAT, exhibited a bell-shaped response with a maximum activity at 0.1 mM $\text{Cd}(\text{NO}_3)_2$. A similar trend was also observed for O_2^- generation. MDA content increased with increasing cadmium concentration in the culture medium, indicating concentration-dependent free radical generation. The SOD activity and MDA levels were well correlated ($r^2 = 0.951$ and $r^2 = 0.990$, respectively) with lower cadmium concentrations (0.01, 0.05, and 0.1 mM). However, the correlation coefficient decreased when the higher cadmium concentration (0.5 mM) was taken into account ($r^2 = 0.462$ and $r^2 = 0.808$) (Figure 6). For low cadmium concentration treatment (0.01 Mm–0.1 mM), the CAT activity and O_2^- were correlated ($r^2 = 0.971$ and $r^2 = 0.837$, respectively) with cadmium concentrations. CAT activity was also well correlated with O_2^- levels ($r^2 = 0.814$) in this case (SI Figures S10 and S11). However, correlations between *P. chrysosporium* CAT activity, O_2^- levels, and $\text{Cd}(\text{NO}_3)_2$ concentration were not observed when the higher cadmium concentration (0.5 mM) was taken into account, because the CAT activity and O_2^- levels of *P. chrysosporium* exposed to 0.5 mM $\text{Cd}(\text{NO}_3)_2$ were much lower than those of *P. chrysosporium* exposed to 0.1 mM $\text{Cd}(\text{NO}_3)_2$.

DISCUSSION

Microbial metabolism is complex, and cells have a wide array of physiological defense mechanisms for survival (e.g., efflux pumps, facultative electron transport, resistance systems).³⁹ Fungi are more resistant to chemical stress following acclimation, and species such as *P. chrysosporium* have the ability to survive in the presence of certain chemical toxic.^{16,40} The growth environment of *P. chrysosporium* is often complex and toxic. Thus, detailed characterization of the interactions

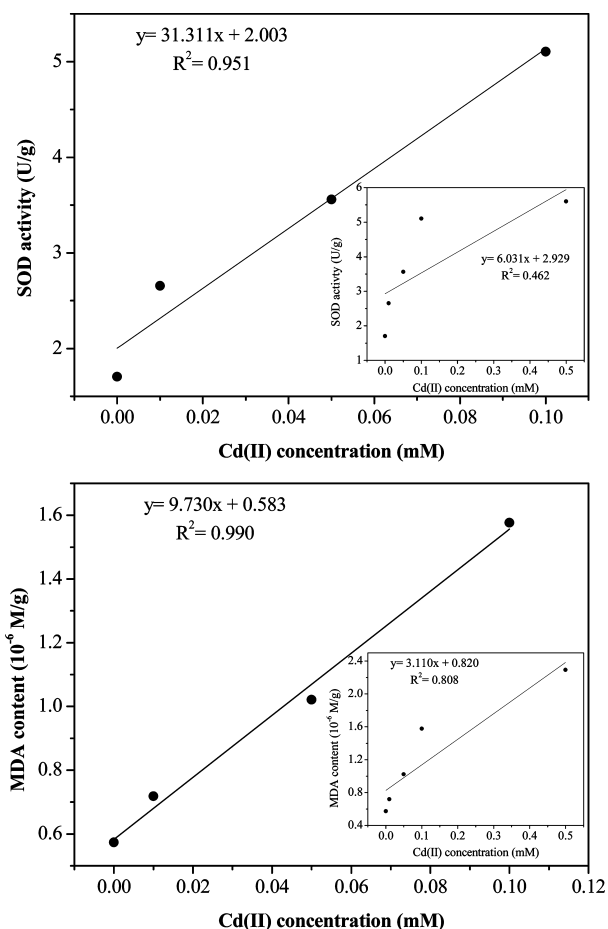


Figure 6. Correlation between *P. chrysosporium* superoxide dismutase (SOD) activity, malondialdehyde (MDA) level, and $\text{Cd}(\text{NO}_3)_2$ concentration in the medium.

between *P. chrysosporium* and toxic pollutants would provide useful information for the development of fungal-based technologies to improve the degradation of metal-polluted organic wastes.

The dynamics of homeostatic H^+ transport/cytoplasmic pH regulation in microorganisms depends on many factors (e.g., local microenvironment, species type, mode of energy transport), and oxygen transport is complicated by facultative respiration.⁴¹ The increased H^+ influx in *P. chrysosporium* was a response to 2,4-DCP-induced oxidative stress. The presence of this toxic pollutant in the medium may alter the bioactivity of the cell or perturb the structure of membrane phospholipids, thereby increasing H^+ permeability across the cytoplasmic membrane.^{42,43} The increased O_2 influx following the addition of 10 mg/L 2,4-DCP is indicative of a possible improvement in respiration. Aromatic compounds can be used as carbon and energy sources for the removal of heavy metals from a medium containing microorganisms.² Our previous study also showed that a low concentration of 2,4-DCP (<20 mg/L) in the medium is beneficial for cadmium removal.³ Thus, the 2,4-DCP (10 mg/L) in this study may be used as a carbon and energy source to improve respiration and increase O_2 influx. The H^+ flux changed from influx to efflux after the addition of 0.1 mM $\text{Cd}(\text{NO}_3)_2$ to the medium. This may be due to the removal of Cd^{2+} from the medium via the bonding of Cd^{2+} to the multiple functional groups on the *P. chrysosporium* mycelial cell wall surface (e.g., $-\text{OH}$, $-\text{COOH}$, and $-\text{NH}_2$). The bonding of

Cd^{2+} to these groups would release H^+ , thereby increasing H^+ efflux. Cd^{2+} in the medium may enter the *P. chrysosporium* cell during the uptake process and boost the fungal production of organic acids, such as oxalic acid,⁴⁴ which may further increase H^+ efflux.

The rapid decrease in O_2 flux following the addition of 0.1 mM $\text{Cd}(\text{NO}_3)_2$ is indicative of a significant decrease in viability. Cadmium is the most toxic heavy metal for all white-rot fungi⁷ and can affect many vital processes. For example, it inhibits growth and reduces fresh biomass, alters morphology, and stimulates the activity of antioxidant enzymes.^{45,46} It is well-known that cadmium has a high affinity for the sulfhydryl groups of proteins and thereby inhibits SH-bearing, redox-regulated enzymes in many cellular processes.^{47,48} Cadmium also binds to and activates calmodulin and plays an important role in Ca^{2+} -dependent regulatory pathways. It may affect cell wall production by inhibiting extracellular Ca^{2+} influx, promoting intracellular Ca^{2+} efflux, and disrupting the cytoplasmic Ca^{2+} gradient.⁴⁹ Cadmium entry into *P. chrysosporium* during the uptake process affects both individual reactions and complex metabolic processes, including inhibition of growth and protein synthesis.⁷ Moreover, Cd^{2+} may cause various types of cellular damage (e.g., Ca^{2+} release, ROS production, and DNA damage) leading to apoptosis.^{8,50,51}

A larger reduction ($30 \pm 1\%$) in Cd^{2+} influx was observed following treatment with 0.1 mM GdCl_3 (Figures 2 and 5), which may be due to shutdown of the uptake pathway by the added GdCl_3 . In research studies on cellular responses to mechanical stimuli, the cell membrane is a major target for the external mechanical forces that act upon a cell. Ion channels play a crucial role in the ionic permeability of biological membranes and are present in all cells tested so far.⁵² Ion channels detect and transduce external mechanical forces into electrical and/or chemical intracellular signals.⁵³ Gadolinium ion (Gd^{3+}), which is a lanthanide, plays an important role in the structure and function of biomembranes. Furthermore, in the ion channels research field, Gd^{3+} is a well-known inhibitor of mechanosensitive ion channels.^{37,54} The presence of sub-millimolar concentrations of gadolinium (Gd^{3+}) in the medium is sufficient to provoke the near-complete inhibition of shock-induced efflux of metabolites such as lactose and ATP in *Escherichia coli* and yeast and ATP in *Streptococcus faecalis*.⁵⁵ Further, in patch-clamp experiments, gadolinium inhibits the giant stretch-activated channels of *E. coli*, *S. faecalis*, and *Bacillus subtilis*. All these data suggest that stretch-activated channels are localized in the cytoplasmic membrane, where they control metabolite flux and play a major role in the response to environmental stress.⁵⁶ The presence of gadolinium (Gd^{3+}) can also directly inhibit Ca^{2+} influx via fusion, which disrupts the Ca^{2+} gradient and causes cellular damage.³⁷ Thus, the added GdCl_3 may decrease Cd^{2+} influx by shutting down the Cd^{2+} uptake pathway (Ca^{2+} channel) and disrupting the Ca^{2+} gradient in *P. chrysosporium* cells.

Figure 3 shows the Cd^{2+} flux of *P. chrysosporium* exposed to 0.1 and 0.5 mM $\text{Cd}(\text{NO}_3)_2$ for different durations. A high concentration of cadmium enhances the driving force for mass transfer to overcome the mass transfer limitation between the *P. chrysosporium* pellets and the fluid phase, thereby increasing the Cd^{2+} influx.⁵⁷ In addition, an elevated cadmium concentration increases the number of collisions between the pellets and Cd^{2+} , thereby enhancing the uptake process.^{58,59} The enhanced uptake reduces the time required to achieve saturation. Thus, following exposure to 0.5 mM $\text{Cd}(\text{NO}_3)_2$ for

1 h, the Cd^{2+} influx dramatically decreased from -121 ± 4 $\text{pmol cm}^{-2} \text{s}^{-1}$ to -5 ± 1 $\text{pmol cm}^{-2} \text{s}^{-1}$, which was lower than that following a 1-h treatment with 0.1 mM $\text{Cd}(\text{NO}_3)_2$. Moreover, a high Cd^{2+} concentration in the medium was likely to have caused extensive damage to the *P. chrysosporium* cells, leading to a decrease in cellular bioactivity.

In our study, enzymatic activities and ROS levels significantly responded to metal exposure. However, the concentration–response relationships were not always monotonic, and, in 2 cases (CAT and O_2^-), bell-shaped concentration–response curves were noted: a significant increase was observed in the lower concentration range (<0.1 mM) and a decline was observed at higher metal concentrations (>0.1 mM). Free radical generation in *P. chrysosporium*, evaluated by MDA production, increased under heavy metal stress (Figure 5), which is similar to the effect of heavy metals in higher plants.^{32,60} This suggests that the toxic effect of heavy metals may be exerted via free radical generation. Heavy metals induce the production of ROS, including superoxide radical (O_2^-), hydrogen peroxide (H_2O_2), and hydroxyl radical (OH^\cdot) and produce a variety of damaging effects collectively termed as oxidative stress.⁶¹ Under normal circumstances, cells can reduce oxygen to water via their electron transport chains and protect themselves from ROS-induced damage by using enzymes such as SOD (to convert superoxide to hydrogen peroxide) and CAT (to convert hydrogen peroxide to water and oxygen).⁶² Under unfavorable conditions such as heavy metal exposure, oxidative stress occurs and the accumulated ROS can rapidly attack biomolecules, including nucleic acids, proteins, lipids, and amino acids, leading to irreparable metabolic dysfunction and cell death.^{31,61}

MDA measurement is used as an indicator of lipid peroxidation, which is linked to the production of O_2^- .⁶⁰ The elevated MDA levels suggest that metal ions stimulate the free radical-generating capacity of the microorganism. The generation of cadmium-induced ROS will stimulate the production of antioxidant enzymes to protect the cellular components from damage. Thus, the increase in SOD activity observed in our study is a response to the elevated MDA levels. SOD activity was well correlated with MDA levels ($r^2 = 0.964$) at low cadmium concentrations (0.01 mM to 0.1 mM). However, when the ROS levels exceed the ability of the antioxidant system to cope with them, cellular damage occurs, indicated by the reduced correlation between SOD activity and MDA levels ($r^2 = 0.873$) (SI Figure S9). Exposure to 0.5 mM $\text{Cd}(\text{NO}_3)_2$ did not elicit an obvious increase in SOD activity, and the CAT activity was lower than that of 0.1 mM $\text{Cd}(\text{NO}_3)_2$. These observations are consistent with the findings of Lichtenthaler⁶³ who described the stress responses of plants as bell-shaped curves and considered the decreasing part as an exhaustion phase in which defense systems are overloaded, leading to chronic damage and cell death. Similarly, the nonlinear and bell-shaped curves observed in this study at high concentrations may reflect cytotoxicity due to ROS overproduction induced by the interactions between excess metals and cellular components. The excess superoxide radical disrupts signaling pathways that activate genes encoding antioxidant enzymes, such as SOD. Similar results were obtained by Dazy et al.⁶⁴ for *Fontinalis antipyretica* Hedw. Although genome/proteome damage was not quantified in the present study, the observed relationships between cellular damage (MDA and O_2^- level) and antioxidant enzyme levels suggest that the tolerance of *P.*

chrysosporium to heavy metals partially depends on its ability to prevent oxidative stress.

Physiological changes are often the earliest events in cellular stress response (e.g., changes in respiration/growth rate/homeostasis), and many of these mechanisms are used by cells to protect the genome/proteome from damage.²² Results from this study will serve as useful references for the physiological responses of fungi to environmental toxic exposure. Further studies combining genomic/proteomic analysis and patch-clamp measurements are required to understand whether changes in physiological transport are linked to global changes in cell viability (genetic damage and mutation) and transmembrane signaling.

■ ASSOCIATED CONTENT

📄 Supporting Information

More details of the noninvasive microtest system; real-time and average changes in H^+ , O_2 , and Cd^{2+} flux at different treatments; correlations among SOD activity, MDA content, CAT activity, O_2^- levels, and $\text{Cd}(\text{NO}_3)_2$ concentration in the medium. This material is available free of charge via the Internet at <http://pubs.acs.org>.

■ AUTHOR INFORMATION

Corresponding Author

*Phone: +86 731 88822829. Fax: +86 731 88823701. E-mail: zgming@hnu.edu.cn (G.Z.), gqchen@hnu.edu.cn (G.C.).

Notes

The authors declare no competing financial interest.

■ ACKNOWLEDGMENTS

This study was financially supported by the National Natural Science Foundation of China (51039001, 51178171, 50908078, 50978088), Program for New Century Excellent Talents in University (NCET-10-0361), the Hunan Key Scientific Research Project (2009FJ1010), and the Hunan Provincial Natural Science Foundation of China (10JJ7005). The authors acknowledge the facilities, and the scientific and technical assistance of the YoungerUSA Non-Invasive Micro-Test Center at Xuyue Science & Technology Co. Ltd. Beijing, China.

■ REFERENCES

- (1) Chen, G.; Zeng, G.; Tang, L.; Du, C.; Jiang, X.; Huang, G.; Liu, H.; Shen, G. Cadmium removal from simulated wastewater to biomass byproduct of *Lentinus edodes*. *Bioresour. Technol.* **2008**, *99* (15), 7034–7040.
- (2) Song, H.; Liu, Y.; Xu, W.; Zeng, G.; Aibibu, N.; Xu, L.; Chen, B. Simultaneous Cr(VI) reduction and phenol degradation in pure cultures of *Pseudomonas aeruginosa* CCTCC AB91095. *Bioresour. Technol.* **2009**, *100* (21), 5079–5084.
- (3) Chen, A.; Zeng, G.; Chen, G.; Fan, J.; Zou, Z.; Li, H.; Hu, X.; Long, F. Simultaneous cadmium removal and 2,4-dichlorophenol degradation from aqueous solutions by *Phanerochaete chrysosporium*. *Appl. Microbiol. Biotechnol.* **2011**, *91* (3), 811–821.
- (4) Fragoero, S.; Magan, N. Enzymatic activity, osmotic stress and degradation of pesticide mixtures in soil extract liquid broth inoculated with *Phanerochaete chrysosporium* and *Trametes versicolor*. *Environ. Microbiol.* **2005**, *7* (3), 348–355.
- (5) Yu, M.; Zeng, G.; Chen, Y.; Yu, H.; Huang, D.; Tang, L. Influence of *Phanerochaete chrysosporium* on microbial communities and lignocellulose degradation during solid-state fermentation of rice straw. *Process Biochem.* **2009**, *44* (1), 17–22.
- (6) Huang, D. L.; Zeng, G. M.; Feng, C. L.; Hu, S.; Zhao, M. H.; Lai, C.; Zhang, Y.; Jiang, X. Y.; Liu, H. L. Mycelial growth and solid-state

fermentation of lignocellulosic waste by white-rot fungus *Phanerochaete chrysosporium* under lead stress. *Chemosphere* **2010**, *81* (9), 1091–1097.

(7) Baldrian, P. Interactions of heavy metals with white-rot fungi. *Enzyme Microb. Technol.* **2003**, *32* (1), 78–91.

(8) Pagès, D.; Sanchez, L.; Conrod, S.; Gidrol, X.; Fekete, A.; Schmitt-Kopplin, P.; Heulin, T.; Achouak, W. Exploration of intracellular adaptation mechanisms of *Pseudomonas brassicacearum* facing cadmium toxicity. *Environ. Microbiol.* **2007**, *9* (11), 2820–2835.

(9) Marco-Urrea, E.; Pérez-Trujillo, M.; Vicent, T.; Caminal, G. Ability of white-rot fungi to remove selected pharmaceuticals and identification of degradation products of ibuprofen by *Trametes versicolor*. *Chemosphere* **2009**, *74* (6), 765–772.

(10) Zeng, G.; Yu, Z.; Chen, Y.; Zhang, J.; Li, H.; Yu, M.; Zhao, M. Response of compost maturity and microbial community composition to pentachlorophenol (PCP)-contaminated soil during composting. *Bioresour. Technol.* **2011**, *102* (10), 5905–5911.

(11) Hartwig, A.; Asmuss, M.; Ehleben, I.; Herzer, U.; Kostelac, D.; Pelzer, A.; Schwerdtle, T.; Bürkle, A. Interference by toxic metal ions with DNA repair processes and cell cycle control: molecular mechanisms. *Environ. Health Perspect.* **2002**, *110* (5), 797–799.

(12) Priester, J. H.; Stoimenov, P. K.; Mielke, R. E.; Webb, S. M.; Ehrhardt, C.; Zhang, J. P.; Stucky, G. D.; Holden, P. A. Effects of soluble cadmium salts versus CdSe quantum dots on the growth of planktonic *Pseudomonas aeruginosa*. *Environ. Sci. Technol.* **2009**, *43* (7), 2589–2594.

(13) Halliwell, B. Oxidative stress in cell culture: an underappreciated problem? *FEBS Lett.* **2003**, *540* (1–3), 3–6.

(14) Ünyayar, S.; Çelik, A.; Çekici, F.; Gözel, A. Cadmium-induced genotoxicity, cytotoxicity and lipid peroxidation in *Allium sativum* and *Vicia faba*. *Mutagenesis* **2006**, *21* (1), 77–81.

(15) Kim, S. J.; Jeong, H. J.; Myung, N. Y.; Kim, M.; Lee, J. H.; So, H.; Park, R. K.; Kim, H. M.; Um, J. Y.; Hong, S. H. The protective mechanism of antioxidants in cadmium-induced ototoxicity in *Vitro* and *In Vivo*. *Environ. Health Perspect.* **2008**, *116* (7), 854–862.

(16) Huang, D. L.; Zeng, G. M.; Feng, C. L.; Hu, S.; Jiang, X. Y.; Tang, L.; Su, F. F.; Zhang, Y.; Zeng, W.; Liu, H. L. Degradation of lead-contaminated lignocellulosic waste by *Phanerochaete chrysosporium* and the reduction of lead toxicity. *Environ. Sci. Technol.* **2008**, *4* (13), 4946–4951.

(17) Iqbal, M.; Eadyvean, R. G. J. Biosorption of lead, copper and zinc ions on loofa sponge immobilized biomass of *Phanerochaete chrysosporium*. *Miner. Eng.* **2004**, *17* (2), 217–223.

(18) Li, Q.; Wu, S.; Liu, G.; Liao, X.; Deng, X.; Sun, D.; Hu, Y.; Huang, Y. Simultaneous biosorption of cadmium (II) and lead (II) ions by pretreated biomass of *Phanerochaete chrysosporium*. *Sep. Purif. Technol.* **2004**, *34* (1–3), 135–142.

(19) Chen, G. Q.; Zhang, W. J.; Zeng, G. M.; Huang, J. H.; Wang, L.; Shen, G. L. Surface-modified *Phanerochaete chrysosporium* as a biosorbent for Cr(VI)-contaminated wastewater. *J. Hazard. Mater.* **2011**, *186* (2–3), 2138–2143.

(20) Costerton, J. W.; Stenmetz, Philip, S.; Greenberg, E. P. Bacterial biofilms: A common cause of persistent infections. *Science* **1999**, *284* (5418), 1318–1322.

(21) Stewart, P. S.; Costerton, J. W. Antibiotic resistance of bacteria in biofilms. *The Lancet* **2001**, *358* (9276), 135–138.

(22) Mclamore, E. S.; Zhang, W.; Porterfield, D. M.; Banks, M. K. Membrane-aerated biofilm proton and oxygen flux during chemical toxin exposure. *Environ. Sci. Technol.* **2010**, *44* (18), 7050–7057.

(23) Denizli, A.; Cihangir, N.; Rad, A. Y.; Taner, M.; Alsancak, G. Removal of chlorophenols from synthetic solutions using *Phanerochaete chrysosporium*. *Process Biochem.* **2004**, *39* (12), 2025–2030.

(24) Kirk, T. K.; Schultz, E.; Connors, W. J.; Lorenz, L. F.; Zeikus, J. G. Influence of culture parameters on lignin metabolism by *Phanerochaete chrysosporium*. *Arch. Microbiol.* **1978**, *117* (3), 277–285.

(25) Lew, R. R.; Levina, N. N. Oxygen flux magnitude and location along growing hyphae of *Neurospora crassa*. *FEMS Microbiol. Lett.* **2004**, *233* (1), 125–130.

(26) Xu, Y.; Sun, T.; Yin, L. P. Application of non-invasive microsensing system to simultaneously measure both H⁺ and O₂ fluxes around the pollen tube. *J. Integr. Plant Biol.* **2006**, *48* (7), 823–831.

(27) Sanchez, B. C.; Ochoa-Acuña, H.; Porterfield, D. M.; Sepúlveda, M. S. Oxygen flux as an indicator of physiological stress in fathead minnow (*Pimephales promelas*) embryos: A realtime biomonitoring system of water quality. *Environ. Sci. Technol.* **2008**, *42* (15), 7010–7017.

(28) Chatni, M. R.; Maier, D. E.; Porterfield, D. M. Evaluation of microparticle materials for enhancing the performance of fluorescence lifetime based optrodes. *Sens. Actuators, B* **2009**, *141* (2), 471–477.

(29) Chatni, M. R.; Porterfield, D. M. Self-referencing optrode technology for non-invasive real-time measurement of biophysical flux and physiological sensing. *Analyst* **2009**, *134* (11), 2224–2232.

(30) Chatni, M. R.; Li, G.; Porterfield, D. M. Frequency-domain fluorescence lifetime optrode system design and instrumentation without a concurrent reference light-emitting diode. *Appl. Opt.* **2009**, *48* (29), 5528–5536.

(31) Choudhary, M.; Jetley, U. K.; Khan, M. A.; Zutshi, S.; Fatma, T. Effect of heavy metal stress on proline, malondialdehyde, and superoxide dismutase activity in the cyanobacterium *Spirulina platensis*-SS. *Ecotoxicol. Environ. Saf.* **2007**, *66* (2), 204–209.

(32) Cavalcanti, F. R.; Oliveira, J. T. A.; Martins-Miranda, A. S.; Viégas, R. A.; Silveira, J. A. G. Superoxide dismutase, catalase and peroxidase activities do not confer protection against oxidative damage in salt-stressed cowpea leaves. *New Phytol.* **2004**, *163* (3), 563–571.

(33) Aravind, P.; Prasad, M. N. V. Zinc alleviates cadmium-induced oxidative stress in *Ceratophyllum demersum* L.: a free floating freshwater macrophyte. *Plant Physiol. Biochem.* **2003**, *41* (4), 391–397.

(34) Lei, Y.; Yin, C.; Li, C. Differences in some morphological, physiological, and biochemical responses to drought stress in two contrasting populations of *Populus przewalskii*. *Physiol. Plant.* **2006**, *127* (2), 182–191.

(35) Lee, J.; Ishihara, A.; Oxford, G.; Johnson, B.; Jacobson, K. Regulation of cell movement is mediated by stretch-activated calcium channels. *Nature* **1999**, *400* (22), 382–386.

(36) Antoine, A. F.; Faure, J. E.; Cordeiro, S.; Dumas, C.; Rougier, M.; Feijó, J. A. A calcium influx is triggered and propagates in the zygote as a wavefront during in vitro fertilization of flowering plants. *Proc. Natl. Acad. Sci. USA* **2000**, *97* (19), 10643–10648.

(37) Antoine, A. F.; Faure, J. E.; Dumas, C.; Feijó, J. A. Differential contribution of cytoplasmic Ca²⁺ and Ca²⁺ influx to gamete fusion and egg activation in maize. *Nat. Cell Biol.* **2001**, *3* (12), 1120–1123.

(38) Ma, W.; Xu, W.; Xu, H.; Chen, Y.; He, Z.; Ma, M. Nitric oxide modulates cadmium influx during cadmium-induced programmed cell death in tobacco BY-2 cells. *Planta* **2010**, *232* (2), 325–335.

(39) Chandran, K.; Love, N. G. Physiological state, growth mode, and oxidative stress play a role in Cd(II)-mediated inhibition of *Nitrosomonas europaea* 19718. *Appl. Environ. Microbiol.* **2008**, *74* (8), 2447–2453.

(40) Yu, Z.; Zeng, G. M.; Chen, Y. N.; Zhang, J. C.; Yu, Y.; Li, H.; Liu, Z. F.; Tang, L. Effects of inoculation with *Phanerochaete chrysosporium* on remediation of pentachlorophenol-contaminated soil waste by composting. *Process Biochem. (Amsterdam, Neth.)* **2011**, *46* (6), 1285–1291.

(41) Muller, J. F.; Stevens, A. M.; Craig, J.; Love, N. G. Transcriptome analysis reveals that multidrug efflux genes are upregulated to protect *Pseudomonas aeruginosa* from pentachlorophenol stress. *Appl. Environ. Microbiol.* **2007**, *73* (14), 4550–4558.

(42) Ray, S.; Peters, C. A. Changes in microbiological metabolism under chemical stress. *Chemosphere* **2008**, *71* (3), 474–483.

(43) Wang, L.; Zhang, J.; Zhao, R.; Zhang, C.; Li, C.; Li, Y. Adsorption of 2,4-dichlorophenol on Mn-modified activated carbon prepared from *Polygonum orientale* Linn. *Desalination* **2011**, *266* (1–3), 175–181.

(44) Jarosz-Wilkolazka, A.; Gadd, G. M. Oxalate production by wood-rotting fungi growing in toxic metal-amended medium. *Chemosphere* **2003**, *52* (3), 541–547.

(45) Errasquín, E. L.; Vázquez, C. Tolerance and uptake of heavy metals by *Trichoderma atroviride* isolated from sludge. *Chemosphere* **2003**, *50* (1), 137–143.

(46) Peña-Castro, J. M.; Martínez-Jerónimo, F.; Esparza-García, F.; Cañizares-Villanueva, R. O. Phenotypic plasticity in *Scenedesmus incrassatulus* (Chlorophyceae) in response to heavy metals stress. *Chemosphere* **2004**, *57* (11), 1629–1636.

(47) Hall, J. L. Cellular mechanisms for heavy metal detoxification and tolerance. *J. Exp. Bot.* **2002**, *53* (366), 1–11.

(48) Poirier, I.; Jean, N.; Guary, J. C.; Bertrand, M. Responses of the marine bacterium *Pseudomonas fluorescens* to an excess of heavy metals: Physiological and biochemical aspects. *Sci. Total Environ.* **2008**, *406* (1–2), 76–87.

(49) Fan, J. L.; Wei, X. Z.; Wan, L. C.; Zhang, L. Y.; Zhao, X. Q.; Liu, W. Z.; Hao, H. Q.; Zhang, H. Y. Disarrangement of actin filaments and Ca^{2+} gradient by CdCl_2 alters cell wall construction in *Arabidopsis thaliana* root hairs by inhibiting vesicular trafficking. *J. Plant Physiol.* **2011**, *168* (11), 1157–1167.

(50) Bleuel, C.; Wesenberg, D.; Sutter, K.; Miersch, J.; Braha, B.; Baerlocher, F.; Krauss, G. J. The use of the aquatic moss *Fontinalis antipyretica* L. ex Hedw. as a bioindicator for heavy metals 3. Cd^{2+} accumulation capacities and biochemical stress response of two *Fontinalis* species. *Sci. Total Environ.* **2005**, *345* (1–3), 13–21.

(51) Weihe, E.; Kriews, M.; Abele, D. Differences in heavy metal concentrations and in the response of the antioxidant system to hypoxia and air exposure in the Antarctic limpet *Nacella concinna*. *Mar. Environ. Res.* **2010**, *69* (3), 127–135.

(52) Gómez-Lagunas, F.; Peña, A.; Liévano, A.; Darszont, A. Incorporation of ionic channels from yeast plasma membranes into black lipid membranes. *Biophys. J.* **1989**, *56* (1), 115–119.

(53) Martinac, B. Mechanosensitive ion channels: molecules of mechanotransduction. *J. Cell Sci.* **2004**, *117* (12), 2449–2460.

(54) Tomoki, T.; Tamba, Y.; Masum, S. M.; Yamashita, Y.; Yamazaki, M. La^{3+} and Gd^{3+} induce shape change of giant unilamellar vesicles of phosphatidylcholine. *BBA, Biochim. Biophys. Acta, Biomembr.* **2002**, *1564* (1), 173–182.

(55) Yang, X. C.; Sachs, F. Block of stretch-activated ion channels in *Xenopus* oocytes by gadolinium and calcium ions. *Science* **1989**, *243* (4894), 1068–1071.

(56) Berrier, C.; Coulombe, A.; Szabo, I.; Zoratti, M.; Ghazi, A. Gadolinium ion inhibits loss of metabolites induced by osmotic shock and large stretch-activated channels in bacteria. *Eur. J. Biochem.* **1992**, *206* (2), 559–565.

(57) Mashitah, M. D.; Azila, Y. Y.; Bhatia, S. Biosorption of cadmium (II) ions by immobilized cells of *Pycnoporus sanguineus* from aqueous solution. *Bioresour. Technol.* **2008**, *99* (11), 4742–4748.

(58) Vimala, R.; Das, N. Biosorption of cadmium (II) and lead (II) from aqueous solutions using mushrooms: A comparative study. *J. Hazard. Mater.* **2009**, *168* (1), 376–382.

(59) Rathinam, A.; Maharshi, B.; Janardhanan, S. K.; Jonnalagadda, R. R.; Nair, B. U. Biosorption of cadmium metal ion from simulated wastewaters using *Hypnea valentiae* biomass: A kinetic and thermodynamic study. *Bioresour. Technol.* **2010**, *101* (5), 1466–1470.

(60) Dhir, B.; Sharmila, P.; Saradhi, P. P. Hydrophytes lack potential to exhibit cadmium stress induced enhancement in lipid peroxidation and accumulation of proline. *Aquat. Toxicol.* **2004**, *66* (2), 141–147.

(61) Choi, O.; Hu, Z. Q. Size dependent and reactive oxygen species related nanosilver toxicity to nitrifying bacteria. *Environ. Sci. Technol.* **2008**, *42* (12), 4583–4588.

(62) Farber, J. L. Mechanisms of cell injury by activated oxygen species. *Environ. Health Perspect.* **1994**, *102* (10), 17–24.

(63) Lichtenthaler, H. K. The stress concept in plants: an introduction. *Ann. N. Y. Acad. Sci.* **1998**, *851* (1), 187–198.

(64) Dazy, M.; Masfaraud, J. F.; Féraud, J. F. Induction of oxidative stress biomarkers associated with heavy metal stress in *Fontinalis antipyretica* Hedw. *Chemosphere* **2009**, *75* (3), 297–302.